NJC

Accepted Manuscript

This article can be cited before page numbers have been issued, to do this please use: C. Torres-Sánchez, A. M. Pérez-López, M. Alqahtani, A. Unciti-Broceta and B. Rubio-Ruiz, *New J. Chem.*, 2018, DOI: 10.1039/C8NJ05704D.

ROYAL SOCIETY OF CHEMISTRY

rsc.li/njc

DOI: 10.1039/C8NJ05704D

Design and manufacture of functional catalyst-carrier structures for the bioorthogonal activation of anticancer agents

Carmen Torres-Sánchez[1*], Ana M. Pérez-López[2], Mohammed N. Alqahtani[1], Asier Unciti-Broceta[2], Belén Rubio-Ruiz[2]

[1]Wolfson School of Mechanical, Electrical and Manufacturing Engineering, Loughborough University, Loughborough, Leicestershire LE11 3TU, UK

[2] Cancer Research UK Edinburgh Centre, Institute of Genetics and Molecular Medicine, The University of Edinburgh, Edinburgh EH4 2XR, UK

Abstract

Novel palladium (Pd)-loaded titanium (Ti) devices with high biocompatibility and catalytic activity were prepared using a range of fabrication methods such as powder metallurgy (i.e. sintering with and without space-holder), sputtering, pulsed laser deposition and supersonic cluster beam deposition. The surface of the Ti-[Pd] devices were physico-chemically characterised to confirm the non-alloyed state of the Pd coating onto the titanium substrate. The Pd thickness was optimised to achieve maximum surface area (i.e. maximum catalytic effect) using the minimum amount of material in each method for cost effective production. The catalytic response of the different Ti-[Pd] devices was evaluated under biocompatible conditions by employing an off-on Pd-activatable fluorescent probe. The most robust coating of Pd was produced by an optimised magnetron sputtering method. The sputtered Ti-[Pd] devices were selected to induce the bioorthogonal uncaging of the anticancer drug Vorinostat from a pharmacologically-inactive Pd-activatable precursor in cancer cell culture, demonstrating the capacity of these devices to mediate a local anti-tumour effect via in-situ release of a clinically approved drug. This approach is the first step towards surgically implantable devices that could facilitate targeting affected areas with high spatial selectivity, improving pharmacological activity and reducing systemic side effects through localised treatment directly at the cancer site.

Keywords

Palladium, Titanium, sputtering, deposition, bioorthogonal catalysis, chemotherapy prodrug

1. Introduction

Efforts to eradicate cancer and improve survival rates have led to initiatives from national health systems promoting earlier diagnosis, more effective screenings and versatile treatments to improve cancer patient prognosis. Despite remarkable advances in overall cancer survival, death rates are increasing for some cancer types, including aggressive liver, pancreas, uterus, lung and brain cancers.[1-3] In order to extend a positive health outcome trend across the entire spectrum of forms of cancer, new therapies and medtech capabilities are needed. Novel cancer treatments, for example immunotherapy [4], proton beam radiation [5], photodynamic therapy [6] or prodrugs activation therapy [7] aim to support or even replace aggressive approaches such as radio- or chemo-therapies, which typically lead to life-threatening secondary effects on patients. Efficacy and cost-effectiveness are issues that still remain and there are opportunities to develop further new propositions.

Bioorthogonal chemistry focuses on the development and application of selective chemical reactions that are compatible with biological environments and do not interfere with the normal functioning of its components.[8, 9] Such reactions are designed to monitor or modulate physiological and pathological processes and can be mediated by two or more mutually-reactive chemical groups or in combination with non-biotic transition metals (e.g. Cu [10, 11], Au [12], Ru [13, 14] or Pd [15, 16]). The use of heterogeneous metal catalysts as bioorthogonal tools is currently under investigation for the activation of systemically administered prodrugs at a determined location in a catalytic manner (Figure 1).[17-20]

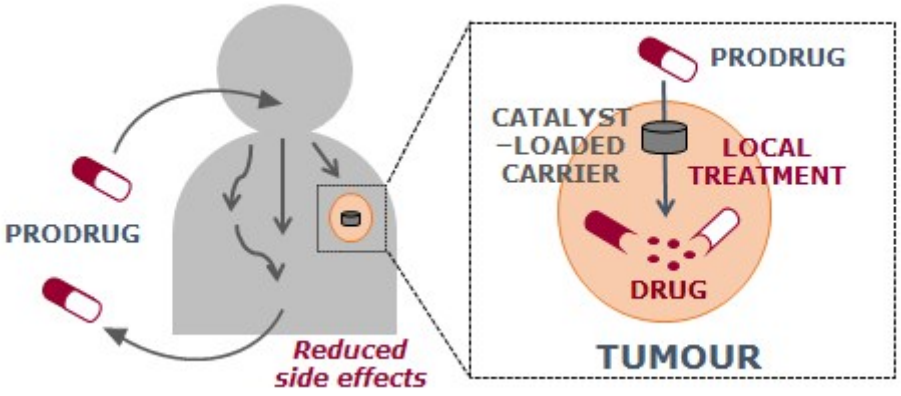

Figure 1: Strategy for the intratumoural activation of inactive prodrug into cytotoxic drugs via catalyst-loaded carriers

Such an experimental therapeutic approach aims to introduce a unique local therapy strategy with the capacity to elicit long-term release of therapeutics in a spatially-controlled fashion within the landscape of

View Article Online
DOI: 10.1039/C8NJ05704D

targeted cancer therapies. As a consequence, the development of novel benign transition metal-loaded devices has been brought into the spotlight in recent years. [11, 21-23] The manufacture of macro scale structures with surfaces containing or coated with such transition metals poses opportunities and challenges. The advantages of a device surgically implantable and detectable using current medical imaging technologies (e.g. titanium metal) could be forfeited by the challenges of manufacturing a metal-catalytic surface that can withstand the stringent physiological conditions inside the body. Metal surfaces and coatings preparation methods such as wet chemistry[24] (e.g. electrostatic adsorption[25] and grafting[26]), vapour- or gas-phase deposition (i.e. chemical[27] and physical[28]), electrochemistry[29] (i.e. electroless and electroplating[30]), plasma or thermal spraying [31] have been previously reported. In this study titanium was used as the substrate and it was coated using palladium element in its unalloyed state, i.e. Pd^0, for catalytic purposes. This transition metal was chosen to profit from the wealth of probes and prodrugs that are activated by Pd chemistry.[17-20, 32, 33] A suitable manufacturing process for the devices had to comply with the following requirements: realisation of highly conformal nano-scale surfaces; achieved at low substrate temperatures to prevent metal alloying or surface oxidation[34]; avoid the use of toxic precursors or intermediates that could contaminate the exposed surface[35] and be both cost and time effective. Powder metallurgy and physical deposition methods were therefore selected on account of their compliance with these processing requirements.

The devices' catalytic efficiency was tested through the uncaging of a prodye (a non-fluorescent compound) to obtain fluorescent Rhodamine 110 dye upon Pd-mediated *O*-depropargylation. The Ti-[Pd] devices were optimised by tailoring their physical features (i.e. shape, dimensions and specific surface area) and chemical composition. Subsequently to investigate their capability as chemotherapeutic drug activator, a bioorthogonal Pd-labile prodrug of the histone deacetylase inhibitor Vorinostat (SAHA), an anticancer drug [20], was incubated with the devices in cancerous cell culture in order to assess its conversion into the active antitumour drug.

2. Materials and Methods

2.1. Materials

Ti powder (Alfa Aesar, USA, -325 mesh, average particle size ≤44 μm, 99.5% purity) and Pd powder (Aldrich Co., UK, -200 mesh, average particle size ≤74 μm, 99.9% purity) were used for the fabrication of

the sintered carriers. NaCl particles (Sigma Aldrich, UK, +80 mesh, average particle size 177 µm, ≥98% purity) were used as space holders to mix with the Pd powder. Prior to that, the NaCl particles were sieved (AS 400 control, Retsch, Germany) and separated into the following size range groups: (i) 45-106 µm; (ii) 106-212 µm; (iii) >212 µm. A final group (iv) of random particles (45-212+ µm) was also used. A Pd disc (PI-Kem Ltd, UK, 57 mm diam, 0.1 mm thickness, 99.99%) was used as target for the sputtering process. A Pd target (Testbourne Ltd, UK, 15x15x2 mm, 99.99%) was used for the pulsed laser deposition process. A Pd rod (Goodfellow, ITA, 6 mm diam, 10 mm length, 99.95%) was used for the supersonic cluster beam deposition method. For the probe/prodrug activation assays, chemicals and solvents such as Rhodamine 110 chloride, *N,N*-dimethylformamide (DMF), Propargyl chloroformate and *N,N*-Diethylethanamine (i.e. trimethylamine) were purchased from Fisher Scientific UK, Sigma-Aldrich or VWR International Ltd. Vorinostat (SAHA) was purchased from Cayman Chemical Co. UK. All chemicals and solvents were >95% pure according to the supplier's information. Synthesized compounds were >95% pure as measured either by HPLC and/or NMR and TLC. NMR spectra were recorded at ambient temperature on a 500 MHz Bruker Avance III spectrometer. Analytical TLC was performed using Merck TLC Silica gel 60 F254 plates and visualized by UV light. Purifications were carried out by flash column chromatography using commercially available silica gel (220-440 mesh, Sigma-Aldrich). Fluorescence signal in the fluorogenic assay and in the reusability study was obtained in a PerkinElmer Victor multilabel spectrophotometer (excitation filter at 480 nm and emissions filter at 535 nm) and is reported in Relative Fluorescence Units (RFU). Fluorescence emission for the cytotoxicity studies was measured using a PerkinElmer Victor multilabel reader (excitation filter at 540 nm and emissions filter at 590 nm). Stock solutions (100 mM) were prepared in biological grade DMSO.

2.2. Sintering method (S)

Pd wafers were prepared using Pd powder only, cold pressed in a 10mm diameter stainless steel die to 20 kN applying a vertical load (Press 40 Specac, Atlas, UK). The Pd wafers were sintered in a vacuum furnace (LTF 1400C, Lenton, USA equipped with a HiCube 80 pump, Pfeiffer, Germany) at 1,000 °C for 1 h and10^{-5} mbar to prevent any oxidation. After natural cooling to room temperature, the wafers were polished (EcoMet250, Buehler, USA) manually using 320 and 1200 grit SiC paper until a shiny finish was achieved. Samples were prepared in triplicate and used without further treatment.

View Article Online
DOI: 10.1039/C8NJ05704D

2.3. Sintering and space holder method (Sx)

Ti powder (0.35 g) was poured into a 10mm diameter mould. Meantime, the Pd powder (0.21 g) was mixed with the space holder (NaCl, 0.09 g) in the four size ranges (Si, Sii, Siii, Siv) in a ratio 2.21 Pd:NaCl to obtain a 70% volumetric nominal porosity. The mixture was poured into the 10 mm diam mould where the Ti powder awaited and then conjointly subjected to cold isostatic pressing (as above, at 25 kN) followed by sintering at 1,000 °C for 1 h in a vacuum furnace (as above) to avoid oxidation of the samples. After natural cooling to room temperature the specimens were profusely washed in distilled water to remove the space holder. Samples were prepared in triplicate in the 4 size ranges of the space holder. The samples were used without further treatment.

2.4. Sputtering method (SP)

A 2 mm height Ti disc was prepared through the same cold isostatic process (as above) using a die of 16 mm diameter and compressing to 250 MPa. This Ti disc was sintered in the vacuum furnace at 1,200 °C for 2 h and $<10^{-5}$ mbar as above. Once the samples had cooled naturally to room temperature these were ground and polished (EcoMet250 and AutoMet250, Buehler, USA) using the following routine applying 15 N of downward force: 320, 600 and 1200 grit SiC paper at 180 rpm and water cooled until flat surface, then 9 μm diamond suspension on a counter-rotating ultra-pad cloth at 120 rpm for 10 min. The final polishing step involved the use of 1 μm colloidal silica using a microcloth pad using the same rotation settings. The sintered and polished Ti discs were sputtered in a Magnetron sputtering system (Q150T ES, Quorum Technologies Ltd, UK) using a pure Pd disc target in the vacuum chamber at 10^{-5} mbar after Ar flushing with a current of 40 mA and sputtering at a pressure of $9x10^{-3}$ mbar . The deposition rate for the coating was set to 21 nm/min to achieve a coating thickness set to 42 nm and to 62.8 nm. Samples were prepared in quadruplicate and used without further treatment.

2.5. Pulsed laser deposition method (PLD)

Ti discs manufactured using the same procedure as above (see 'Sputtering method' section) were mounted onto a bespoke stainless steel holder and placed in the laser chamber, designed to perform deposition on large areas. More details on the process have been reported. [36] The chamber was heated to 120 °C, vacuum

flushed and left to cool down naturally to room temperature (24-48 h), which created a base pressure of 10^{-9} mbar. The Pd target was placed 10 cm distant from the sample, and the laser (840 mW, GCR-5 solid state Q-switched Nd:YAG, Polaron C V T Ltd., UK & IFW Dresden, GE) emitted 10 pulses/s with visible light at 532 nm wavelength. The coating on each sample was aimed to be 65 nm and it took 2.5 h to complete. The samples were prepared in duplicate and used without further treatment.

2.6. Supersonic cluster beam deposition method (SCBD)

Ti discs manufactured using the same procedure as above (see 'Sputtering method' section) were treated with this method, devised for microstructured metallisation of surfaces, at Prof M Milani's lab (University of Milano, Italy) following the process previously described. [37] Using a Pd rod as target, Pd clusters were formed in the gas phase using a pulsed microplasma source, expanded through a nozzle to generate a supersonic gas stream and deposited at a typical rate of 0.5 nm/min on the Ti discs in vacuum at10^{-7} mbar with an aimed mean film thickness of 42 nm (as measured by the quartz microbalance). The samples were tested without any further treatment.

2.7. Screening of devices' surface chemical properties

Synthesis of bis-*N,N'*-propargyloxycarbonyl-rhodamine 110 (prodye). The prodye was synthesised according to literature procedure.[17] Briefly, rhodamine 110 chloride was dissolved in dry DMF under nitrogen atmosphere. Separately, propargyl chloroformate and triethylamine were added dropwise to the mixture. The reaction mixture was stirred at room temperature for 48 h and then purified by chromatographic column. The spectral data matched the values reported in the literature.[17] Purity was >95% measured by TLC and NMR

Fluorogenic assay (prodye-to-dye conversion). The prodye, which presents its fluorescence properties quenched, was used to determine the catalytic efficiency of the Ti-[Pd] devices previously manufactured. They were set in 22x40 mm glass vials. A solution of prodye (100 μM) in PBS (pH = 7.4) was prepared and 2 mL were added to each vial containing Ti-[Pd] devices. The mixtures were stirred at 250 rpm using a magnetic-stirring-bar at 37 °C in an oil bath. The release of Rhodamine 110 was measured after 24 h by fluorescence at $\lambda_{ex/em}$= 480/535 nm.

View Article Online
DOI: 10.1039/C8NJ05704D

Reusability study. Ti-[Pd] devices were taken carefully with flat tweezers and were washed in 5 mL distilled water. The manufactured devices were set in a new 22x40 mm glass vials. A 2 mL fresh solution of prodye at 100 μM in PBS (pH = 7.4) was added to each vial containing the device. The mixtures were stirred at 250 rpm using a magnetic-stirring-bar at 37 °C in an oil bath. The release of Rhodamine 110 (mechanism described in Figure 5) was detected after 24 h of treatment by fluorescence. This cycle was repeated 5 times.

Synthesis of *O*-(4-Propagyloxybenzyl) suberoylanilidehydroxamate (prodrug POB-SAHA). *O*-(4-Propagyloxybenzyl) suberoylanilide hydroxamate (namely POB-SAHA thereafter) was synthesised by treatment of SAHA with 4-(propargyloxy)benzyl bromide and 1,8-diazabicyclo[5.4.0]undec-7-ene at room temperature for 24 h according to literature procedure.[20] ^{1}H-NMR, ^{13}C-NMR and HPLC analyses matched with literature.[20]

2.8. Biological 'in vitro' studies of the surfaces: cytotoxicity and prodrug activation

Cell culture. Human lung adenocarcinoma A549 cells (kindly donated by Dr Simon Wilkinson, University of Edinburgh, UK) were cultured in Dulbecco's Modified Eagle Media (DMEM) supplemented with serum (10% FBS) and L-glutamine (2 mM) and incubated in a tissue culture incubator at 37 °C and 5% CO_2.

Preparation of Ti-[Pd] devices for biological testing. A set of 6 discs of 3 mm of diameter and 2 mm in height manufactured using the SP method were sterilized in an autoclave at 121 °C for 20 min and under UV light for 10 min before treatment.

Cytotoxicity study: The cytotoxicity of the SP Ti-[Pd] devices to the cells was assessed using a PrestoBlue™ cell viability assay against A549 cells. The Prestoblue™ viability assay contains a cell permeable resazurin-based solution that functions as a cell viability indicator by using the reducing power of living cells to quantitatively measure their proliferation. SP Ti-[Pd] devices were cultured in a 24-well plate with 20,000 cells/well for 72 h. Untreated cells were used as control. At that time point Prestoblue™ reagent was added into each well according to the manufacturer's protocol. The plate then was incubated at 37 °C in humidified atmosphere for 120 min. Fluorescence emission was detected at $\lambda_{ex/em}$= 540/590 nm. The test was performed in triplicate.

Activation of prodrug (POB-SAHA) catalysed by SP Ti-[Pd] devices in cancer cell culture and tolerability study. A549 cells were seeded in a 24-well plate format (at 20,000 cells/well) and incubated for

24 h before Pd-mediated activation tests. Media was then aspirated and the SP Ti-[Pd] devices carefully placed onto the surface of each well. Cells were treated with prodrug POB-SAHA (100 μM) or SAHA (100 μM) accordingly and incubated for 72 h. This concentration was selected according to previous reported results.[20] Cells treated with only DMSO (0.1% v/v) were used as control. All experiments were performed in triplicate. PrestoBlue™ cell viability reagent (10% v/v) was added to each well and the plates were incubated for 120 min. Fluorescence emission was measured as explained in the previous section. All conditions were normalized to the untreated cells (100%) and data analysed using GraphPad Prism.

2.9. Characterisation

The surface area of the Pd-carrying devices was measured using a metrology protocols (3D micro coordinate InfiniteFocus, Alicona, Austria) with x5 magnification and using a polarised light with vertical and horizontal resolution of 3.22 μm and 7.82 μm, respectively. A field emission scanning electron microscope SEM/EDS (TM3030/JSM-7800F, Hitachi, Japan) was employed to inspect the surface and to determine the elemental composition of the samples, including the detection of any contamination on the surfaces. X-ray diffraction (benchtop 2phase diffractometer r, Bruker, Germany) tests were conducted at room temperature using a Cu K-alpha source, 30 kV, 20 mA radiation and 0.020 °/step to assess the crystal structure of the Pd deposited and to identify any episode of alloying. X-ray Photoelectron Spectroscopy (K-Alpha XPS, Thermo Scientific, UK) using monochromatic Al Kα radiation micro-focussed to a spot size of 200 μm in 5 μm steps was used to identify the electronic state of the elemental composition and also any Pd oxide contaminant present using a constant analyser energy mode (CAE) at 200 eV pass energy for elemental spectra. Elemental quantification was done with standard single element sensitivity factors using the Thermo Advantage software (TA Instruments, UK). The main photoelectron peaks considered were Pd 3d, C 1s, O 1s, Na1s, Ti 2p and N 1s. XPS was also employed to assess layer thickness using an Al anode (beam diameter 400 μm, power 36 W). XPS depth profiling was done using a 0.5keV argon ion beam, over an area of 2×2 mm and a drilling rate of 0.0878 nm/min, calibrated on a Ta_2O_5 substrate. X-ray fluorescence (Orbis PC Micro-XRF Analyzer, EDAX, USA) equipped with an Rh tube for 50 kV and 50 W was used to assess coating thickness using 5 places on the sample systematically (i.e. centre, top, bottom, left and right), and Atomic Force Microscopy (AFM, Veeco Explorer, USA) was used to confirm such measurements using a Si cantilever (AFM probe-Bruker TESP-MT) applying a force of 20-80 N/m at 330 kHz of resonance frequency. The

scans were conducted at three randomly identified locations and the images analysed using the XEI 1.8 software (Park Systems, South Korea). A Focused Ion Beam (FIB-SEM) system (Nova200 NanoLab, FEI, US) was used to obtain thin slices of the samples in order to measure the thickness of the Pd coating using SEM images.

3. Results

Substrates of titanium coated with metallic palladium (Pd^0) or palladium-only discs were manufactured using powder metallurgy and physical deposition methods to create implantable devices that possess a conformal, stable surface for high-yield catalytic reactions. The devices were physico-chemically characterised. Having confirmed the devices displayed sufficient structural integrity and were of an adequate size for handling, the main feature of interest was the existence and quantity of Pd^0 species on its surface. Crystallographic (i.e. XRD) results from S samples presented a single Pd cubic state element with no other accompanying peak. The manufactured samples (Sx, SP, PLD and SCBD) (Figure 2) showed the presence of both Ti and Pd species in their cubic state. The Sx series presented, in addition, Ti_xO_x compounds.

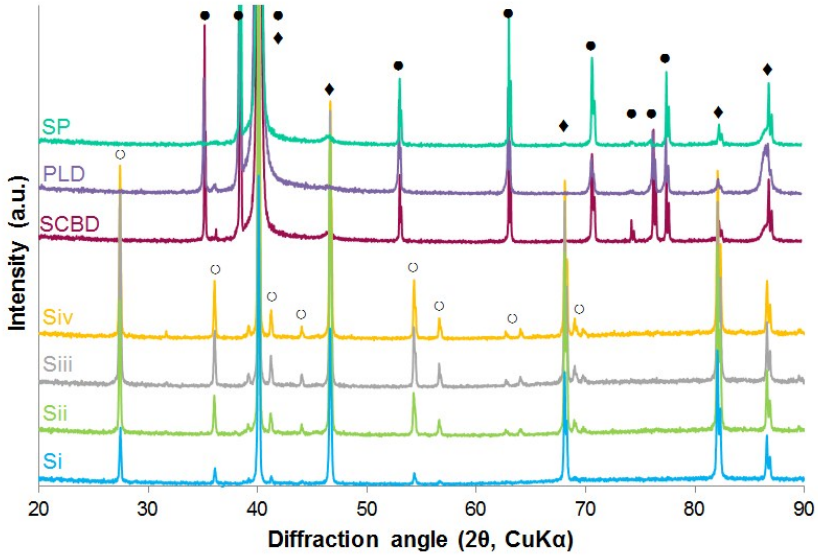

Figure 2: XRD comparison for the Ti-[Pd] devices manufactured using the different methods (♦: Pd; ●: Ti; ○: TiO_2)

Results from XPS tests (Figure 3) showed 2 dominating peaks at 335.33 ± 0.06 eV ($Pd3d_{5/2}$) and 340.85 ± 0.26 eV($Pd3d_{3/2}$), confirming the presence of Pd in its metallic form and with no PdO formed (which would appear with shifted peaks at 337.3 eV ($Pd3d_{5/2}$) and 342.5 eV ($Pd3d_{3/2}$) respectively). An additional peak at

View Article Online
DOI: 10.1039/C8NJ05704D

530.3 eV, which corresponds to the O1s peak resolved for the oxygen present on PdO [38, 39] would have appeared, but the present study shows peaks at 527 and 562 eV instead (those corresponding to that of the background signal, not to the formation of PdO). A C layer, whose (C1s) peak appeared at binding energy 284 eV, which corresponds to the sp2 carbon peak, was present but its intensity decreased after 2 cycles of Ar etching, confirming it was only superficial contamination. Further enquiries over an Ag peak at 366 eV (Ag3d), which corresponded to AgBr, and a Br peak at 68.9 eV, corresponding to Br but also overlapping Na2s, appeared to belong to the background signal. Sintered Pd wafers (S) (Figure 3, insert) presented a dominating peak of C1s with respect to the Pd3d peak expected.

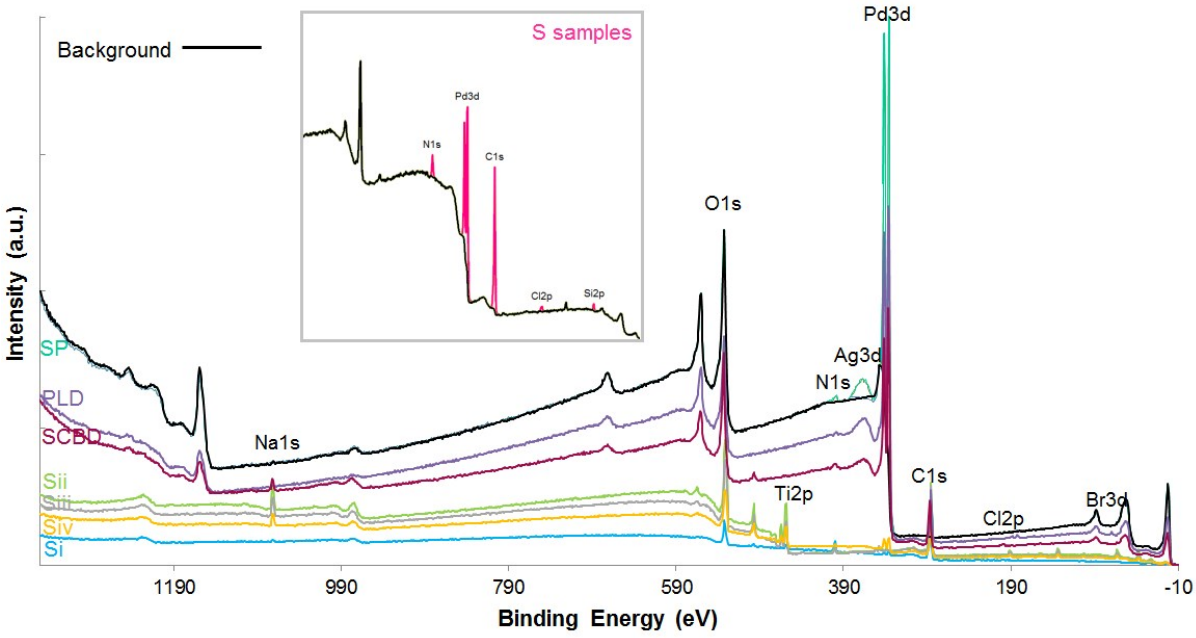

Figure 3: XPS survey spectra for the Ti-[Pd] devices surface manufactured using the different methods under study (inset: 190-590eV range for S samples)

The surface area values obtained are reported in Table 1, along with the mass of Pd deposited on each of the samples manufactured using the different methods in this study. The primary thickness measurement procedure was XRF, and these measurements were confirmed with results from AFM and/or FIB-SEM techniques (Figure 4). The mass of the Pd for the sintered (S) and sintered with space holder (Sx) devices was the amount of Pd powder used in their manufacture, and for the magnetron sputtered (SP), pulsed laser deposition (PLD) and supersonic cluster beam deposition (SCBD) methods this mass was calculated from

View Article Online
DOI: 10.1039/C8NJ05704D

the surface area, the thickness of the Pd coating and the Pd density (12.02 kg/m^3, as per manufacturer's data). The ratio (mm^2/g) gives an indication of the spread of the Pd on the surface on each scaffold.

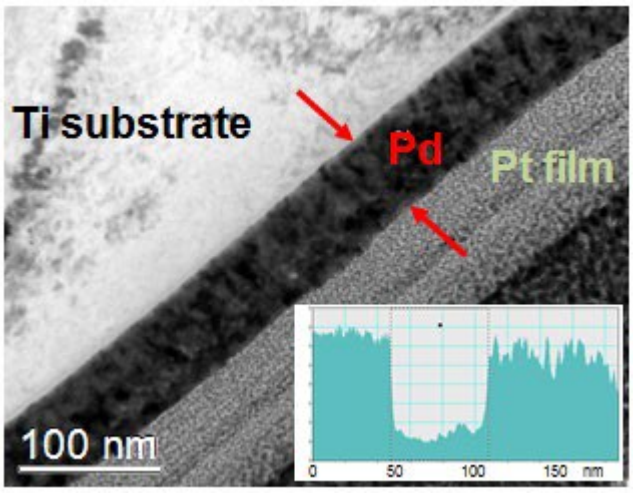

Figure 4: SEM micrograph of the FIB slice displaying the Pd coating sandwiched between the Ti substrate and the support film (Pt) for the cutting operation, and the measurement thereafter (inset)

Table 1: Measured surface area and mass of Pd for the Ti-[Pd] devices manufactured using the methods under study

Manufacturing method	Sample	Surface Area (mm^2) (SD)	Thickness of Pd coating (nm)	Mass of Pd (SD)	Ratio A(mm^2):W(g) (SD)
Sintering (S)	Pd wafer	142.013 (6.039)†	n/a	0.162 g (0.014)	876.624 (80.459)
Sintering with space holder on Pd layer (S_x)					
S_i	Size range: 45-106 µm	147.577 (6.842)	n/a	0.210 g (0.005)	702.748 (36.626)
S_{ii}	106-212 µm	144.835 (26.095)	n/a	0.209 g (0.007)	692.990 (126.995)
S_{iii}	>212 µm	135.560 (11.960)	n/a	0.206 g (0.001)	658.058 (120.594)
S_{iv}	random	114.095 (12.445)	n/a	0.209 g (0.000)	545.909 (59.545)
Sputtering (SP)	Sintered Ti base/Pd coating	172.322 (6.251)	67.600 (3.226) [65.028]^{AFM} [66.706]$^{FIB/SEM}$	0.138 mg (0.005)	1248.710 e^3 (62.658 e^3)
Pulsed Laser Deposition (PLD)	Sintered Ti base/Pd coating	187.43 (12.093)	69.085 (1.515) [66.30]^{AFM}	0.153 mg (0.001)	1225.033 e^3 (112.579 e^3)
Supersonic cluster beam deposition (SCBD)	Sintered Ti base/Pd coating	212.550 (7.640)	50.76 (14.75) [50.5]^{AFM}	0.130 mg (0.038)	1635.000 e^3 (481.523 e^3)

†Total surface area, including both sides
[..]$^{AFM\ or\ FIB/SEM}$, thickness confirmed using these methods

View Article Online
DOI: 10.1039/C8NJ05704D

The catalytic efficiency of the Ti-[Pd] devices to convert the non-fluorescent prodye into green fluorescent Rhodamine 110 was determined by spectrofluorometry (Figure 5). Fluorescence intensity (RFU) values obtained from each of the devices are reported in Figure 5a. To obtain a better picture of the efficacy of each of the devices, RFU values were also normalised with respect to the mass of Pd present on the surface of each device surface as well as the ratio surface area to mass of Pd (Figure 5b).

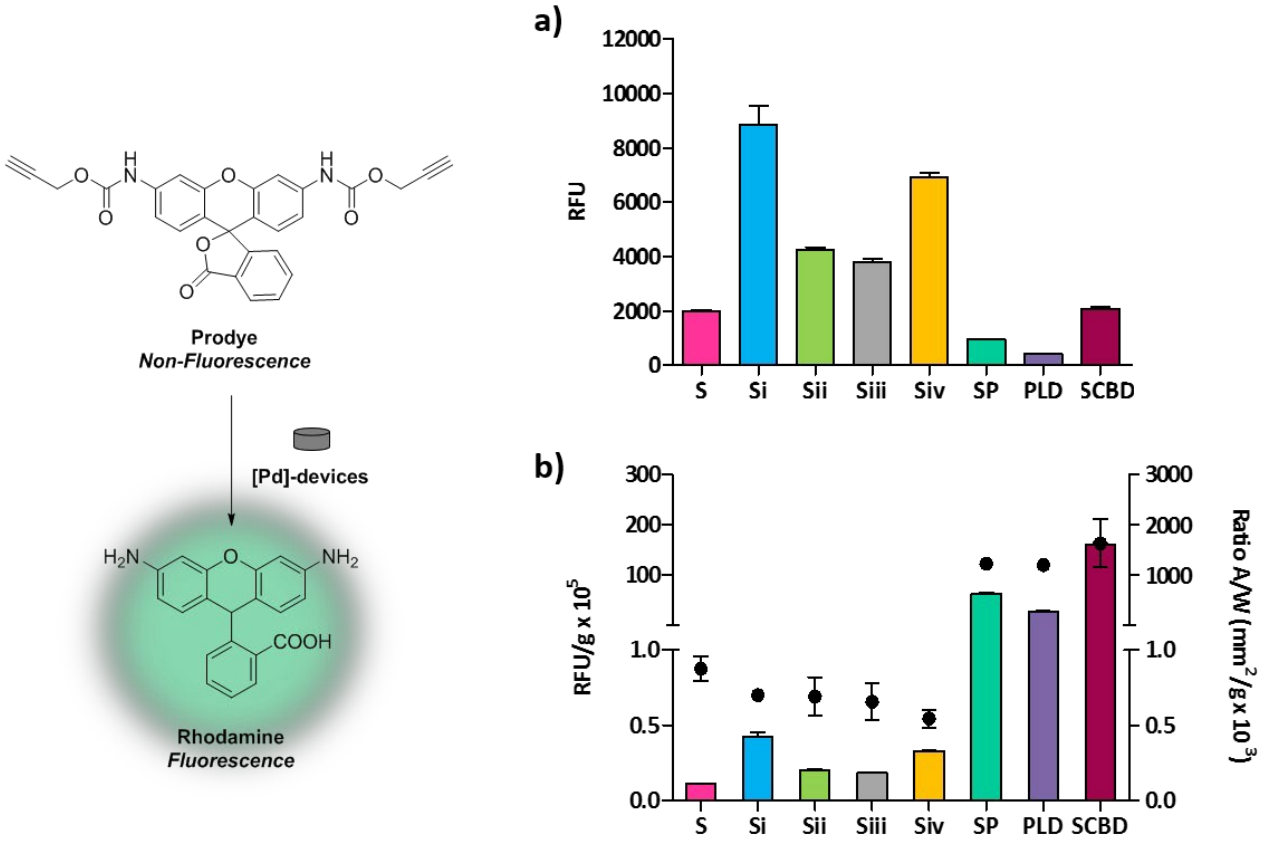

Figure 5: Fluorogenic assay used to determine the catalytic properties of the Ti-[Pd] devices surface. Catalytic efficiency reported as: a) Fluorescence signal obtained for Ti-[Pd] devices after incubation for 24h with the non-fluorescence probe in physiological conditions; b) normalised RFU/g values compared against Surface Area/Pd mass ratio of each device

The results from the reusability study (i.e. 5 cycles of the fluorogenic assay) are shown in Figure 6 and are reported in the normalised format with regards to the amount of Pd mass on the device. This test permitted the assessment of each manufacturing method attending to the Ti-[Pd] devices' catalytic potency when subjected to sequential catalytic reactions.

View Article Online
DOI: 10.1039/C8NJ05704D

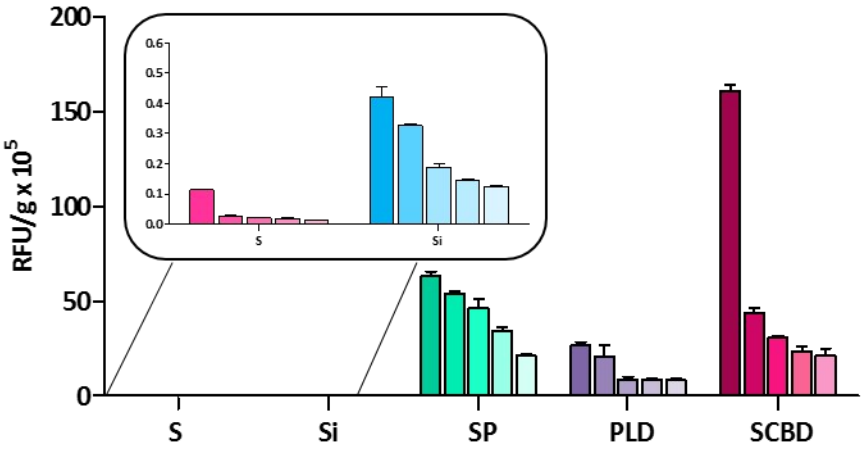

Figure 6: Reusability study of catalytic deprotection of the surface to 5 cycles presented left to right using the Prodye in PBS for 24h on each Ti-[Pd] device manufactured via the different methods

Figure 7 shows SEM analysis on the samples before and after the fluorogenic tests. The images obtained after the tests on the SP, PLD and SCBD samples present evident effects of chipping and pitting, suggesting degradation and detachment of the Pd coating over the cycles. This effect was evaluated through a study on the elemental composition of the Pd film using XPS data on the prevalence of the Pd3d metal species (Table 2), which informed on the amount of Pd^0 available for the fluorogenic assay on the pristine samples (Table 2, 'before' row), as well as through reusability tests using the prodye-into-dye conversion (Table 2,'after').

Table 2: Elemental study on the samples, reported as atomic %, of the main species (incl. Pd3d metal availability for the biochemical tests and C1s, O1s content on the surface along with other minor species) as pristine samples ('before') and as-used samples ('after')

Sample series	Before biochemical tests (atomic %) (SD)						After biochemical tests (atomic %) (SD)						
	Pd3d	C1s	O1s	Na1s	Ti2p	N1s	Pd3d	C1s	O1s	Na1s	Ti2p	N1s	Si2p
S	75.325 (0.095)	26.156 (13.977)	20.552 (13.596)	-	-	6.659 (2.508)	2.535 (0.655)	60.25 (7.870)	20.900 (9.095)	-	-	3.671 (1.879)	16.971 (4.367)
Sx	36.105 (9.525)	33.943 (5.866)	18.931 (14.348)	3.370 (2.970)	5.790 (3.470)	7.010 (1.876)	6.120 (9.428)	44.907 (9.857)	28.995 (8.843)	4.151 (2.740)	8.845 (3.390)	-	-
SP	76.045 (2.535)	23.362 (8.019)	14.462 (10.464)	-	-	7.630 (1.081)	15.865 (1.345)	65.82 (18.334)	16.630 (11.332)	-	-	5.500 (2.340)	3.492 (2.577)
PLD	44.435 (4.865)	37.133 (5.269)	12.163 (6.548)	1.411 (0.876)	-	-	10.540 (1.310)	62.021 (10.333)	30.324 (10.002)	-	-	2.833 (1.909)	-
SCBD	55.770 (25.260)	35.837 (7.498)	14.591 (12.750)	4.079 (2.055)	-	8.831 (3.045)	4.825 (3.925)	36.83 (12.977)	34.595 (13.474)	3.836 (2.899)	23.105 (16.775)	-	-

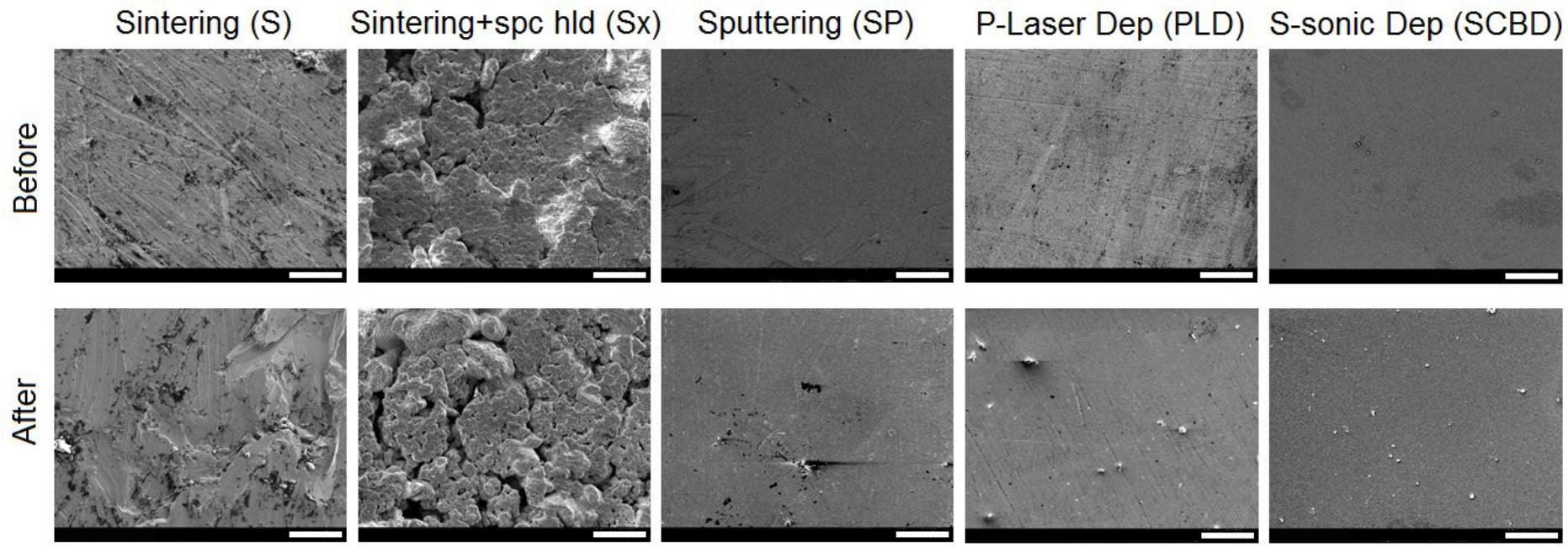

Figure 7: SEM surface images of Ti-[Pd] devices manufactured using the different methods reported before (top row) and after (bottom row) the prodye-to-dye catalytic deprotection tests (scale bar 20 μm)

Given the superior catalytic properties of the SP Ti-[Pd] discs these were selected for the biological studies. Cell cytotoxicity was studied by direct incubation of lung carcinoma A549 cells with the SP Ti-[Pd] discs for 3 days and compared to untreated control cells. Cell viability was quantified via the Prestoblue™ assay. The results shown in Figure 8 demonstrate no cytotoxicity induced by the SP Ti-[Pd] devices. Treatment of the A549 cells with the prodrug POB-SAHA (inactive) in the absence of the devices did not show cytotoxic activity and yielded a cell viability rate close to those of the control. In contrast, the A549 cells incubated with the prodrug POB-SAHA in the presence of the SP Ti-[Pd] discs displayed poor levels of tolerability. Cell viability dropped to the same levels obtained by direct treatment with the active drug SAHA, demonstrating the in-situ uncaging of POB-SAHA by the Ti-[Pd] devices.

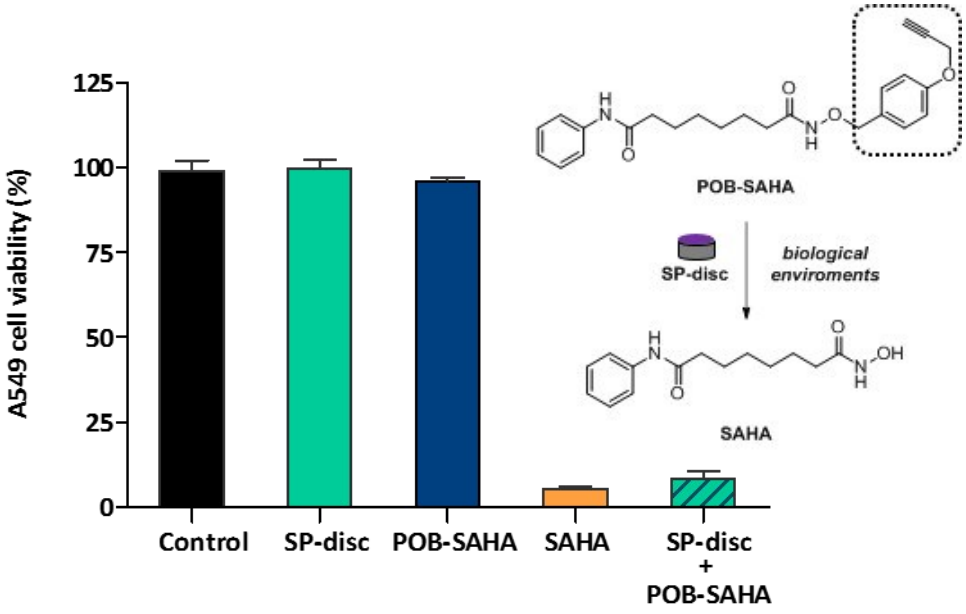

Figure 8: Cell viability and tolerability studies using the Ti-[Pd] device surface to activate prodrug (POB-SAHA) to active antitumour drug (SAHA) in the presence of the Ti-[Pd] device (SP discs+ POB-SAHA, hatched green), compared to untreated cells control (black), cells treated only with SP Ti-[Pd] device (SP discs, green), cells treated only with POB-SAHA (negative control, blue), and cells treated with SAHA (positive control, orange)

4. Discussion

The use of implantable devices with a catalytically active surface to enable focused and localised anticancer therapies is not a new concept.[40-43] One of such technologies are carmustine-containing Gliadel™ wafers, which are used clinically for postsurgical treatment of brain tumours.[44] These devices are however limited by

View Article Online
DOI: 10.1039/C8NJ05704D

their cargo capacity, being rendered useless once the drug content has been released. Catalyst-loaded devices have been recently proposed as an alternative to resolve this issue. Transition metals such as Pd are optimal to mediate continuous catalytic manufacture of bioactive small molecules in living systems and, consequently, different kinds of Pd-functionalized materials have been investigated in recent years.[15, 20, 45] The novelty presented in this work lies in the strategy deployed by the chosen device, a functionalised Ti scaffold whose surface possesses bioorthogonally catalytic capabilities through the incorporation of Pd on the top layer of the device. Shape-ability is an important feature to aid implantation procedures since the size and location of the targeted tissue may present anatomical challenges. While a range of techniques deriving from evaporation methods (e.g. plasma-assisted atomic layer deposition[46]) have been developed to counteract the limitations posed when depositing high surface energy products, such as Pd, onto non-wettable substrates, such as Ti[47], only those based on the physical deposition of the coating were pertinent to this study. Furthermore, the manufacturing processes considered in this work allowed for freedom in the device's construct utilising the minimum amount of raw Pd required, thus lowering the device's production cost, and maximising its surface area and availability of metallic Pd (Pd^0) for an effective catalytic reactivity when in contact with the Pd-sensitive molecules. Several methods for the design and manufacture of these catalyst-loaded carriers were studied, using Titanium as the carrier due to its biocompatibility and contrast-agent properties [48], which could facilitate tracking during the implantation of the device and monitoring throughout the treatment. Loading of the catalyst onto the carrier was addressed to increase the device's catalytic bioactivation activity. Manufacturing methods tested included powder metallurgy (i.e. sintering with and without space holder to increase roughness and therefore increase surface area) and other coating deposition methods explored to develop highly conformal thin coatings and active surfaces: magnetron sputtering, pulsed laser deposition and supersonic cluster beam deposition. A strict control on the specific surface area, minimising the weight to volume ratio, and a high purity of the catalyst, helped to enhance the catalytic activity the Ti-[Pd] devices. A study of the thickness of Pd^0 coated on the titanium substrate demonstrated that methods such as magnetron sputtering, pulsed laser and supersonic cluster beam deposition achieved the thinnest of the coating Pd^0 layers, making these the most cost effective way of creating catalytic-active devices.

View Article Online
DOI: 10.1039/C8NJ05704D

The results from XRD studies (Figure 2) show that alloying between the Ti and Pd did not occur in any of the manufactured devices and the Pd element was retained in its cubic form. The passivating layer of titanium oxide formed on the Ti surface helped avoiding the alloying with the Pd. The Sx series presented TiO_2, whose formation was promoted by the presence of NaCl in the sintering stage through a chloride route.[49] The existence of Na1s peaks in the XPS analysis are remains from the space holder that contaminated the exposed surface. For this reason, along with their poor performance with regards to the surface area:Pd mass ratio and the decreased reusability potency beyond the 3rd cycle, the Sx series specimens were discarded as devices suitable for the application.

Studies on the surface using XPS results further assisted in the assessment of the S samples (Figure 3, inset and Table 2). Large standard deviation (SD) in the XPS spectra values of pristine samples indicate the susceptibility of the surface to attract O1s and C1s species of organic nature (i.e. pollution) after Ar etching the surface. Their large mass and the presence of a substantial C layer (C1s peak) made them less reactive to the catalytic deprotection. These are the only substrate-less samples (without Ti) and although this can be initially seen as an advantage from a lean manufacturing viewpoint, their production cost is the highest of all the series, which renders them less attractive for the application. They also performed poorly in the reusability tests, failing to retain any catalytic potency beyond the 2nd cycle, and the Si2p peak present after the tests is attributed to other contaminants on the surface.

According to the position of the Pd3d peak and its intensity on the XPS spectra performed on the SP, PLD and SCBD Ti-[Pd] devices, the chemical state of metallic Pd was confirmed in these devices. SP were the devices that exhibited the highest of Pd3d peak intensity and SCBD the ones with the least retention presenting a significant amount of Ti2p post tests, depleted of Pd^0 coating. The quantification of the O1s peaks has been reported in Table 2 and these peaks correspond to the organic (i.e. background) C-O and C=O compounds which proved difficult to eliminate despite plasma etching during the XPS analysis. The presence of Na1s peaks can be tracked down to the manufacturing route of the raw Ti powder which is the main constituent of the substrate.[49]

The results from the fluorogenic studies correlated well with the on-surface tests performed on the Ti-[Pd] devices. Despite the SCBD devices generating the highest fluorescence signal when compared to SP and

PLD devices, the surface SEM images obtained after the test presented clear signs of chipping and detachment of the coating (Figure 7, last column). This was confirmed with the results from the reusability tests, with a marked reduction in catalytic activity after the 1st cycle, and by the surface exploration after the tests (Table 2). Concurrently, it can be observed that the Ti-[Pd] devices manufactured using the PLD method show a plateaued fluorogenic signal after the 1st cycle and compared to the successive ones (Figure 6). These results show depletion in catalytic-deprotection activity after the 2nd cycle and are symptomatic of poor integrity of the substrate and its coating.

The SP Ti-[Pd] devices surface reported a higher fluorogenic signal, sustained over the reusability tests, and given the smaller quantities of Pd used, their production is therefore more cost-effective. Consequently, it was concluded that the magnetron sputtering method (SP) was the best manufacturing route to functionalise the devices in a facile, reliable and faster manner. This method allowed the preparation of catalyst-loaded devices with good reusability results, probably due to good adhesion strength at the Pd|Ti interface and highly conformal coating. This result is in agreement with previous work.[50] Therefore, these SP Ti-[Pd] devices were selected for the cell-based studies.

Their potential application to modulate the spatiotemporal generation of a chemotherapeutic drug from an inactive precursor was assessed in cell culture conditions. A 3-day cytotoxicity study confirmed full biocompatibility of the SP Ti-[Pd] devices in human lung carcinoma cell culture. The prodrug POB-SAHA, a completely inactive derivate of the histone deacetylase inhibitor SAHA that is susceptible to deprotection in the presence of Pd^0, was combined in a A549 cell culture with the Ti-[Pd] devices. This combination elicited a potent cytotoxic effect, unequivocal evidence that the active drug is rapidly released in standard cell culture conditions. As previously reported, the mechanism of POB-SAHA deprotection catalyzed by Pd proceeds via *O*-depropargylation of a phenolic ether group followed by spontaneous 1,6-elimination of the *p*-hydroxybenzyl intermediate.[20] Treatment of A549 cells with POB-SAHA (negative control) manifested no effect on the cells, while cells treated with SAHA (positive control) induced widespread cell mortality (Figure 8).[51]

5. Conclusions

Due to the lack of selectivity and unwanted side effects of current chemotherapies, the design of drug-eluting devices that can be implanted inside tumours to release cytotoxic agents only at the disease site is an important area of research. Local therapy technologies (e.g. drug-eluting implants) can reduce systemic side effects of chemotherapy treatments but are restricted by a limited loading capacity. Once the drug content is released in full, the devices become obsolete. To solve this limitation, we have developed a novel Pd-coated Ti carriers with catalytic surfaces as implantable "activating" devices which are innocuous but capable of mediating the spatiotemporal generation of chemotherapeutic drugs from an inactive precursor in cell culture conditions. With stringent design specifications determining the manufacture of the device, several fabrication processes were investigated and the surface performance of the products assessed with regards to their structural integrity, production costs and efficacy on a fluorogenic assay that informed of the bioorthogonal uncaging potency of the Ti-[Pd] devices. Cell based studies with the best-performing type of devices (i.e. magnetron sputtered) demonstrated the full biocompatibility and capacity to synthesise in-situ a clinically used drug in lung cancer treatment (i.e. SAHA). This capacity is tightly correlated to the functionalised surface of the device and the availability of Pd in its metallic form (Pd^0). The results from this study confirmed the selection of a protocol that fulfils the design requirements, could aid mass customisation of catalyst-loaded carriers and permits a cost-effective production of these devices that could take us a step closer towards achieving continuous intratumoural release of anticancer drugs in the clinic.

Conflict of interest

The authors declare no conflict of interest.

Acknowledgements

CT-S acknowledges the support from the EPSRC Platform Grant Embedded Integrated Intelligent Systems for Manufacturing (EP/P027482/1). AP-L and AU-B are grateful to the EPSRC (EP/N021134/1) for funding. BR-R thanks the EC (H2020-MSCA-IF-2014-658833, ChemoBOOM) for financial support. MA was funded by the Cultural Bureau of the Royal Embassy of Saudi Arabia in London (no. JU64). CT-S and MA are grateful to the staff at the Loughborough Materials Characterisation Centre for sample analysis and to Dr T Santaniello for SCBD sample preparation.

References:

View Article Online
DOI: 10.1039/C8NJ05704D

1. R. L. Siegel, K. D. Miller and A. Jemal, *Ca-Cancer J. Clin.*, 2016, **66**, 7-30.
2. R. De Angelis, M. Sant, M. P. Coleman, S. Francisci, P. Baili, D. Pierannunzio, A. Trama, O. Visser, H. Brenner, E. Ardanaz, M. Bielska-Lasota, G. Engholm, A. Nennecke, S. Siesling, F. Berrino and R. Capocaccia, *Lancet Oncol.*, 2014, **15**, 23-34.
3. W. Chen, R. Zheng, P. D. Baade, S. Zhang, H. Zeng, F. Bray, A. Jemal, X. Q. Yu and J. He, *Ca-Cancer J. Clin.*, 2016, **66**, 115-132.
4. D. M. Pardoll, *Nature Reviews Cancer*, 2012, **12**, 252.
5. J. Lundkvist, M. Ekman, S. R. Ericsson, B. Jönsson and B. Glimelius, *Acta Oncologica*, 2005, **44**, 850-861.
6. D. E. J. G. J. Dolmans, D. Fukumura and R. K. Jain, *Nature Reviews Cancer*, 2003, **3**, 380.
7. W. A. Denny, *European Journal of Medicinal Chemistry*, 2001, **36**, 577-595.
8. D. M. Patterson, L. A. Nazarova and J. A. Prescher, *ACS Chemical Biology*, 2014, **9**, 592-605.
9. E. M. Sletten and C. R. Bertozzi, *Angewandte Chemie International Edition*, 2009, **48**, 6974-6998.
10. J. Clavadetscher, S. Hoffmann, A. Lilienkampf, L. Mackay, R. M. Yusop, S. A. Rider, J. J. Mullins and M. Bradley, *Angewandte Chemie International Edition*, 2016, **55**, 15662-15666.
11. Y. Liu, S. Pujals, P. J. M. Stals, T. Paulöhrl, S. I. Presolski, E. W. Meijer, L. Albertazzi and A. R. A. Palmans, *Journal of the American Chemical Society*, 2018, **140**, 3423-3433.
12. A. M. Perez‐Lopez, B. Rubio‐Ruiz, V. Sebastian, L. Hamilton, C. Adam, T. L. Bray, S. Irusta, P. M. Brennan, G. C. Lloyd‐Jones, D. Sieger, J. Santamaria and A. Unciti‐Broceta, *Angewandte Chemie (International Ed. in English)*, 2017, **56**, 12548-12552.
13. C. Streu and E. Meggers, *Angewandte Chemie International Edition*, 2006, **45**, 5645-5648.
14. M. Tomás-Gamasa, M. Martínez-Calvo, J. R. Couceiro and J. L. Mascareñas, *Nature Communications*, 2016, **7**, 12538.
15. J. Li, J. Yu, J. Zhao, J. Wang, S. Zheng, S. Lin, L. Chen, M. Yang, S. Jia, X. Zhang and P. R. Chen, *Nature Chemistry*, 2014, **6**, 352.
16. R. M. Yusop, A. Unciti-Broceta, E. M. V. Johansson, R. M. Sánchez-Martín and M. Bradley, *Nature Chemistry*, 2011, **3**, 239.
17. J. T. Weiss, J. C. Dawson, K. G. Macleod, W. Rybski, C. Fraser, C. Torres-Sánchez, E. E. Patton, M. Bradley, N. O. Carragher and A. Unciti-Broceta, *Nature Communications*, 2014, **5**, 3277.
18. J. T. Weiss, J. C. Dawson, C. Fraser, W. Rybski, C. Torres-Sánchez, M. Bradley, E. E. Patton, N. O. Carragher and A. Unciti-Broceta, *Journal of Medicinal Chemistry*, 2014, **57**, 5395-5404.
19. J. T. Weiss, N. O. Carragher and A. Unciti-Broceta, *Scientific Reports*, 2015, **5**, 9329.
20. B. Rubio-Ruiz, J. T. Weiss and A. Unciti-Broceta, *Journal of Medicinal Chemistry*, 2016, **59**, 9974-9980.
21. G. Y. Tonga, Y. Jeong, B. Duncan, T. Mizuhara, R. Mout, R. Das, S. T. Kim, Y.-C. Yeh, B. Yan, S. Hou and V. M. Rotello, *Nature Chemistry*, 2015, **7**, 597.
22. M. A. Miller, B. Askevold, H. Mikula, R. H. Kohler, D. Pirovich and R. Weissleder, *Nature Communications*, 2017, **8**, 15906.

23. M. Hoop, A. S. Ribeiro, D. Rösch, P. Weinand, N. Mendes, F. Mushtaq, X. Z. Chen, Y. Shen, C. F. Pujante, L. J. Puigmartí, J. Paredes, B. J. Nelson, A. P. Pêgo and S. Pané, *Advanced Functional Materials*, 2018, **28**, 1705920.
24. H. Yoneyama, N. Nishimura and H. Tamura, *The Journal of Physical Chemistry*, 1981, **85**, 268-272.
25. Q. Dong, T. Yin, H. Wan, G. Zhu, G. Yu and C. Guo, *Int J Electrochem Sci*, 2016, **11**, 804-814.
26. S. Verma, R. B. Nasir Baig, M. N. Nadagouda and R. S. Varma, *Tetrahedron*, 2017, **73**, 5577-5580.
27. A. Niklewski, T. Strunskus, G. Witte and C. Wöll, *Chemistry of Materials*, 2005, **17**, 861-868.
28. B. Amin-Ahmadi, H. Idrissi, M. Galceran, M. S. Colla, J. P. Raskin, T. Pardoen, S. Godet and D. Schryvers, *Thin Solid Films*, 2013, **539**, 145-150.
29. *US Grant Pat.,* US Grant US5149420A. 1992.
30. I. Ohno, in *Modern Electroplating*, eds. M. Schlesinger and M. Paunovic, John Wiley & Sons, Inc., Fifth edn., 2010, ch. 20, pp. 477-482.
31. T. Boeltken, D. Soysal, S. Lee, G. Straczewski, U. Gerhards, P. Peifer, J. Arnold and R. Dittmeyer, *Journal of Membrane Science*, 2014, **468**, 233-241.
32. C. Adam, A. M. Pérez-López, L. Hamilton, B. Rubio-Ruiz, T. L. Bray, D. Sieger, P. M. Brennan and A. Unciti-Broceta, *Chemistry – A European Journal*, 2018, **24**, 16783-16790.
33. T. L. Bray, M. Salji, A. Brombin, A. M. Pérez-López, B. Rubio-Ruiz, L. C. A. Galbraith, E. E. Patton, H. Y. Leung and A. Unciti-Broceta, *Chemical Science*, 2018, **9**, 7354-7361.
34. T. Aaltonen, M. Ritala, Y.-L. Tung, Y. Chi, K. Arstila, K. Meinander and M. Leskelä, *Journal of Materials Research*, 2004, **19**, 3353-3358.
35. D. N. Goldstein and S. M. George, *Thin Solid Films*, 2011, **519**, 5339.
36. S. J. Guilfoyle, M. D. Crapper, M. Lovelady and M. Petty, *Journal of Magnetism and Magnetic Materials*, 1999, **198-199**, 113-115.
37. R. Luca, D. Giorgio, R. Sara, M. Mattia, P. Paolo and M. Paolo, *Journal of Physics D: Applied Physics*, 2009, **42**, 082002.
38. M. Peuckert, *The Journal of Physical Chemistry*, 1985, **89**, 2481-2486.
39. A. I. Titkov, A. N. Salanov, S. V. Koscheev and A. I. Boronin, *Reaction Kinetics and Catalysis Letters*, 2005, **86**, 371-379.
40. O. A. Ali, N. Huebsch, L. Cao, G. Dranoff and D. J. Mooney, *Nature materials*, 2009, **8**, 151-158.
41. T. Garg, O. Singh, S. Arora and R. S. R. Murthy, 2012, **29**, 1-63.
42. S.-H. Lee and H. Shin, *Advanced Drug Delivery Reviews*, 2007, **59**, 339-359.
43. M. Schuler, D. Trentin, M. Textor and S. G. Tosatti, *Nanomedicine*, 2006, **1**, 449-463.
44. J. Perry, A. Chambers, K. Spithoff and N. Laperriere, *Current Oncology*, 2007, **14**, 189-194.
45. B. W. Michel, A. R. Lippert and C. J. Chang, *Journal of the American Chemical Society*, 2012, **134**, 15668-15671.
46. M. J. Weber, A. J. M. Mackus, M. A. Verheijen, V. Longo, A. A. Bol and W. M. M. Kessels, *The Journal of Physical Chemistry C*, 2014, **118**, 8702-8711.
47. G. N. Smolenskaya and N. T. Kudryavtsev, *Metal Science and Heat Treatment of Metals*, 1960, **2**, 615-616.
48. S. G. Orel and M. D. Schnall, *Radiology*, 2001, **220**, 13-30.
49. P. Sun, H. Liu, H. Yang, W. Fu, S. Liu, M. Li, Y. Sui, Y. Zhang and Y. Li, *Applied Surface Science*, 2010, **256**, 3170-3173.
50. S.-J. Ding, *Biomaterials*, 2003, **24**, 4233-4238.

51. V. M. Richon, *British Journal of Cancer*, 2006, **95**, S2-S6.

View Article Online
DOI: 10.1039/C8NJ05704D

View Article Online
DOI: 10.1039/C8NJ05704D

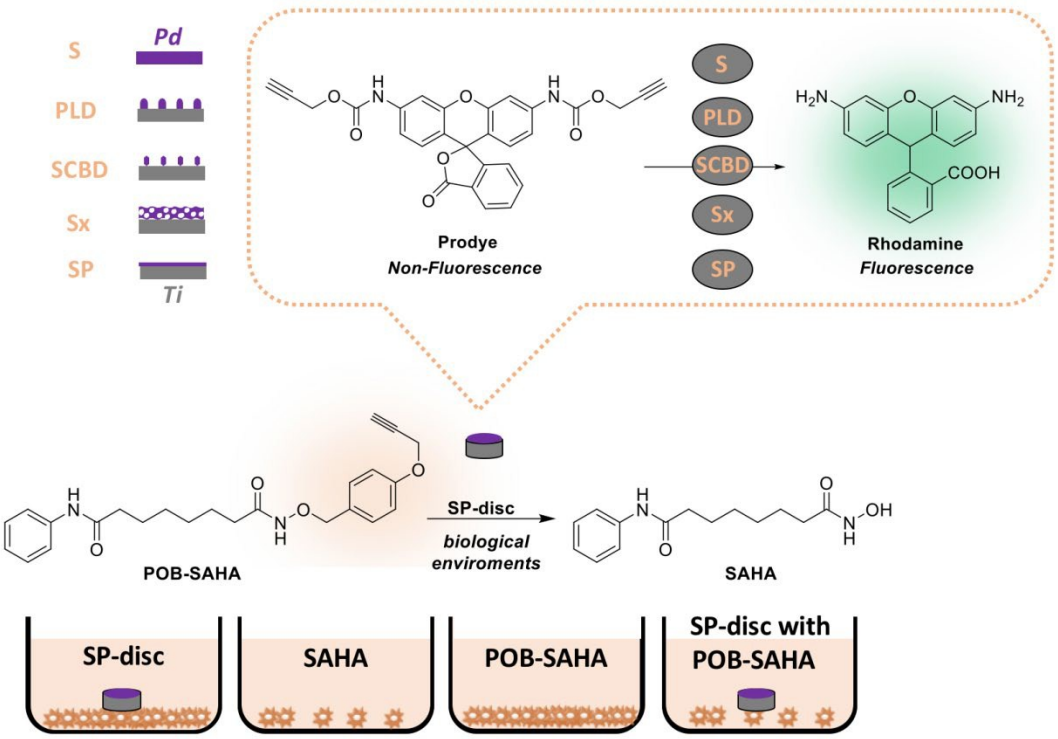

Achieving the activation of a latent prodrug via bio-orthogonal chemistry on the catalytic surface of a tailored Ti-[Pd] device